Macromolecular Research

Article

DOI 10.1007/s13233-018-6022-3

www.springer.com/13233 pISSN 1598-5032 eISSN 2092-7673

Characteristics of Polycarbonate Composites with Poly(methyl methacrylate) Grafted Multi-Walled Carbon Nanotubes

Eun Yeob Choi
Jeong Ung Nam
So Hyun Hong
Chang Keun Kim*

School of Chemical Engineering & Materials Science, Chung-Ang University, 221 Huksuk-dong, Dongjak-gu, Seoul 06974, Korea

Received April 11, 2017 / Revised October 19, 2017 / Accepted October 26, 2017

Abstract: To improve the mechanical strength and electrical conductivity of polycarbonate (PC)-based composites with multi-walled carbon nanotubes (MWCNT), poly(methyl methacrylate) (PMMA)-grafted MWCNT (PMMA-MWCNT) was first prepared by polymerizing the monomer MMA on MWCNT that was functionalized with 3-(trimethoxysily)propylmethacrylate. A composite of PC and MWCNT was then produced by melt extrusion to examine its mechanical properties; another composite was also fabricated from solution to explore the dispersion of MWCNT and the electrical conductivity. The measured adhesion energy of the PC and PMMA-MWCNT was the highest value that could be obtained with PC and MWCNT, which guaranteed the strongest adhesion and the most uniform dispersion of the MWCNT in the composite. When compared to the PC/MWCNTs composite, the PC composite with PMMA-MWCNT exhibited improved interfacial adhesion and dispersion of the MWCNT, resulting in better mechanical and electrical properties.

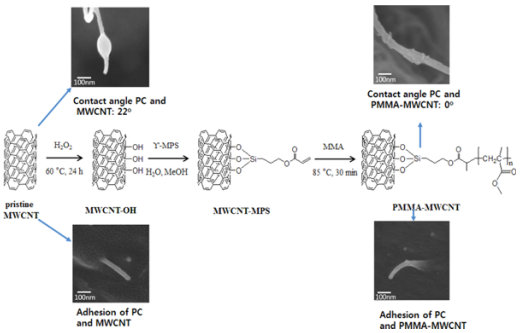

Keywords: polycarbonate, poly(methyl methacrylate) grafted multi-walled carbon nanotube, composites, interfacial adhesion, tensile strength.

1. Introduction

Carbon nanotubes (CNT) have been widely explored for application as a reinforcement material in polymer composites because of their excellent inherent properties.[1,2] Polymer composites containing CNT are expected to have an immense technological and commercial impact because the composites are expected to have superior electrical conductivity and mechanical strength.[3-5] However, there is a limit to the development of composites with superior properties owing to CNT entanglement and poor adhesion at the interface of CNT and polymers. Moreover, CNTs easily aggregate because of the strong interactions among them and their high aspect ratio.[4,5] To overcome these problems, many techniques, including CNT functionalization with organic moieties and polymer grafting on CNT, have been developed to prepare composites of CNTs and polymers.[5-11]

Bisphenol-A polycarbonate (PC) has received much attention because of its high thermal resistance, impact strength, and transparency.[12] PC is widely used in many industrial fields, including housings of electrical devices and automotive parts, but its use is often limited by its low mechanical strength and issues related to electrostatic dissipation.[13,14] These weaknesses of PC might be overcome by blending with CNT. The preparation of an effective filler for reinforcement and electrostatic dissipation requires fine CNT dispersion and excellent adhesion at the PC and CNT interface. The PC composites with modified CNTs have been explored for this purpose.[4-11] For example, CNTs that were functionalized with hydroxyl, carboxylic acid, and acyl halides and CNTs that were grafted with polymers were prepared. Examination of composites of these modified CNTs and PC revealed mechanical and electrical properties that were improved from those of composites of PC and pristine CNTs.

Polymer grafting onto CNT can be a more effective strategy than CNT functionalization in improving mechanical and electrical properties of the PC/CNT composite because of the inevitable chain entanglement between the grafted polymer and matrix polymer. Composites of PC and poly(styrene-*co*-acrylonitrile) (SAN)-grafted CNT have been studied,[7] but effective chain entanglement between PC and SAN might not be feasible because of their immiscibility.[15,16]

In this study, poly(methyl methacrylate) (PMMA)-grafted multi-walled carbon nanotubes (MWCNTs), hereafter referred to as PMMA-MWCNT, were prepared by radical polymerization, and the properties of their composites with PC were explored. It is known that PMMA is nearly miscible with PC.[17,18] A higher level of chain entanglement at the interface between PC and MWCNTs is expected because of the miscibility of PC with PMMA. The adhesion energies at the PC and MWCNT interface were calculated by analyzing the shape of PC droplets formed on the MWCNT. The electrical conductivity and mechanical strength of the PC composites with MWCNT were also examined.

Acknowledgments: This research was supported by the Fundamental R&D Program for Technology of World Premier Materials funded by the Ministry of Knowledge Economy, Republic of Korea. This researchwas also supported by the Chung-Ang University Excellent Student Scholarship.

***Corresponding Author:** Chang Keun Kim (E-mail: ckkim@cau.ac.kr)

2. Materials

The MWCNTs (JC-170, average length: 1.7 μm, average diameter: 13 nm) were supplied by Jeio Co. (Seoul, Korea). Polycarbonate (GP-100L, $\overline{M}_n$ =22,000 g/mol, $\overline{M}_w$ =43,000 g/mol) that was synthesized by interfacial polymerization between bisphenol-A and phosgene was purchased from LG Chemicals (Seoul, Korea). Hydrogen peroxide (H_2O_2) and 3-(trimethoxysily)propylmethacrylate (g-MPS) was used as reactants to functionalize MWCNTs, ammonium hydroxide was used as a catalyst for the coupling reaction between the hydroxyl terminated MWCNT and γ-MPS; *n*-hexane, methanol, and tetrahydrofuran (THF) were used as solvents; these reactants, catalyst, and solvents were supplied by Sigma-Aldrich. Methyl methacrylate (MMA) was used as the monomer for the synthesis of PMMA that would be grafted on MWCNTs and azobisisobutyronitrile (AIBN) was used as an initiator for polymerization; both them were purchased from Junsei Chemicals (Tokyo, Japan).

3. Experiment

3.1. Fabrication and characterization of modified MWCNTs

The route for the fabrication PMMA-MWCNT is shown in Figure 1. First, MWCNTs containing hydroxyl groups (MWCNT-OH) were prepared by reacting MWCNT and H_2O_2. The aqueous solution (500 mL) containing 25 mol% of H_2O_2 and 0.5 g of MWCNT was heated to 60 °C and then left for the components to react for 24 h to form the MWCNT functionalized with hydroxyl groups. The resulting MWCNTs were collected by vacuum filtration. The MWCNT-MPS, which contained carbon-carbon double bonds as chain end-groups, was prepared through the reaction between MWCNTs-OH and γ-MPS. An aqueous solution (deionized water: 40 mL) containing methanol (10 mL) and ammonium hydroxide (0.1 mol) was mixed with MWCNT-OH at 30 °C for 30 min under sonication. After γ-MPS (4 g) was added to the aqueous solution, the reaction proceeded at 80 °C for 12 h.

To prepare the PMMA-MWCNT, AIBN (0.2 g) was added to MMA (100 mL) containing MWCNT-MPS (0.5 g). The polymerization reaction then proceeded at 80 °C for 30 min. Note that the concentration of converted MMA remained at 10 wt%. THF (300 mL) was added to the product and then the resulting MWCNTs were collected by vacuum filtration. This process was repeated seven times to completely separate ungrafted PMMA and remaining MMA.

The structure of the modified MWCNTs was analyzed by Fourier-transform infrared (FT-IR; Magna 750, Nicolet, Wisconsin, USA) spectra and X-ray photoelectron spectra (XPS; VG Microtech, ESCA2000, UK). The morphologies of various MWCNTs and their composites with PC were observed with high-resolution transmission electron microscopy (HR-TEM; JEM 2000EXII, JEOL, Tokyo, Japan) and field-emission scanning electron microscopy (FE-SEM; Sigma, Carl Zeiss, Oberkochen, Germany). The amount of PMMA in the PMMA-MWCNT was estimated with a thermogravimetric analyzer (TGA; TGA-2050, TA Instruments, Newcastle, Delaware, USA) under purging nitrogen.

3.2. Preparation and characterization of composites

The preparation of composites containing PC and MWCNTs was described in our previous work.[19] The PC and MWCNT composites were produced by melt extrusion using a twin extruder (BA-11, Bau, Seoul, Korea) with a length-to-diameter ratio of 40. The temperatures of the feeding zone, melting zone, mixing zone, and exit die of the twin extruder were 260, 280, 300, and 300 °C, respectively. The extruded composites were immersed in water and then pelletized with a chopper. Injection molding was performed to prepared tensile specimens (specification ASTM D-638). The pelletized composite was dried in an air-circulating oven at 100 °C for 2 h before injection molding. The temperatures of the mixing zone and the nozzle of the injection molding machine were 280 and 290 °C, respectively. The tensile properties of the specimens were measured with a universal testing machine (UTM-301, R&B Co, Daejon, Korea) at a cross-head speed of 5 mm/min. The average tensile values calculated from the testing results with seven specimens were reported.

The composite films were fabricated by solvent casting to examine the MWCNT dispersion in the composites and the electrical conductivities of the composites. The MWCNTs were dispersed in a THF solution containing PC (5 wt% of THF) under sonication. The resulting solution was poured onto a glass plate and cast with a casting knife with thickness of 200 μm. The resulting film was dried in a vacuum oven at 100 °C for 24 h after most of the solvent had evaporated in an air-circulating oven at 50 °C for 24 h. The electrical conductivities of the composites fabricated by solvent casting were measured by the four-point probe method.

The adhesion energies of PC and various MWCNTs were calculated from the PC contact angles on MWCNTs using Young's equation.[20] The details obtaining adhesion energy from the contact angle were previously reported.[9,11,21-23] The contact angle was evaluated by analyzing the PC droplet-shape generated on the MWCNTs. To generate a PC droplet on a MWCNT, a THF (200 mL) solution that consisted of PC (10 mg) and MWCNTs (10 mg) was precipitated using *n*-hexane as a nonsolvent. The PC-covered MWCNTs were recovered by vacuum-filtration

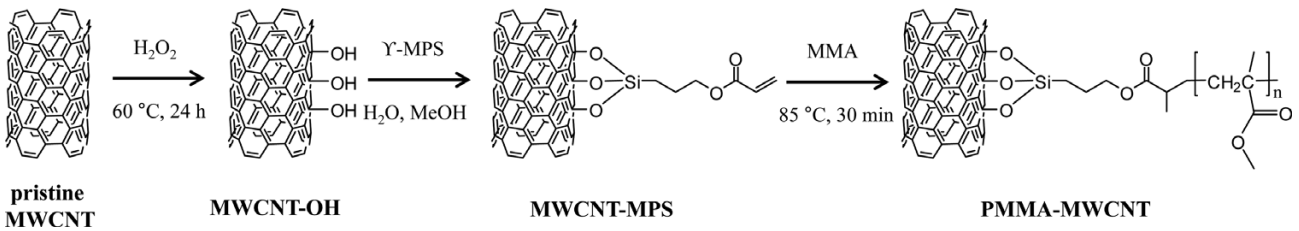

Figure 1. Synthesis route for PMMA-MWCNT.

and annealed at 310 °C for 30 min to form PC droplets. The PC droplets encapsulating MWCNT were observed with the FE-SEM to obtain its contact angle on the MWCNT surface. The average value of the contact angles measured from five droplets was reported.

4. Results and Discussion

4.1 Characteristics of the modified MWCNTs

The FT-IR spectra of MWCNT and MWCNT functionalized with the hydroxyl groups were almost the same, with both showing a peak at 3405 cm^{-1} originated from the hydroxyl groups and a peak at 1650 cm^{-1} originated from sp^2 carbon in the MWCNTs, as shown in Figure 2. MWCNT contains carbon and oxygen atom as listed in Table 1. Oxygen atoms in MWCNT existed in the forms of oxygen containing functional groups such as carbonyl and hydroxyl groups.[24] The characteristic peaks originating from

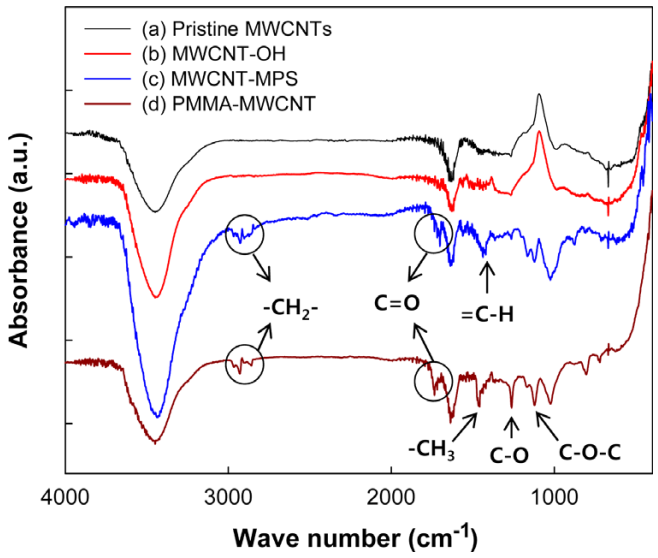

Figure 2. The IR spectra of pristine and modified MWCNTs.

Table 1. Atomic mole ratios of pristine and modified MWCNTs

	C1s	O1s	Si2p
pristine MWCNT	98.25	1.75	0
MWCNT-OH	93.89	6.11	0
MWCNT-MPS	89.27	7.78	1.07
PMMA-MWCNT	84.43	13.02	0.60

C-H stretching vibration of methylene groups (2850-2950 cm^{-1}) and carbonyl groups (1715 cm^{-1}), which do not appear in the spectrum of the MWCNT functionalized with the hydroxyl groups, were observed in the MWCNT-MPS spectrum. The features originated from C=C in γ-MPS (1640 cm^{-1}) and sp^2 carbon in the MWCNTs (1650 cm^{-1}) appear at similar positions. As shown in Figure 2, all peaks originating from PMMA are present in the PMMA-MWCNT spectrum.

Figure 3 presents XP spectra of pristine and modified MWCNTs; the atomic ratios calculated from Figure 3 are listed in Table 1. A C1s peak and an O1s peak were observed in all spectra, and a Si2P peak that originated form γ-MPS was observed in the MWCNT-MPS and PMMA-MWCNT spectra. The ratio between the O1s and C1s peaks in the spectrum of MWCNT-OH (6.1:93.9) was greater than that in the spectrum of pristine MWCNTs (1.8:98.2) because of hydroxyl groups on the MWCNT-OH. The molar fraction of Si-O groups in the MWCNT-MPS (1.1%) was greater than that of the PMMA-MWCNT (0.6%) because of the PMMA grafting.

Figure 4 shows TGA thermograms of PMMA, MWCNT, and PMMA-MWCNT. The MWCNT did not undergo thermal degradation until 800 °C. PMMA and the PMMA-MWCNT first experienced thermal degradation at 260 and 305 °C, respectively. The thermal degradation of PMMA originated from a homolytic chain scission of vinyl groups,[25] which could decelerate owing to the PMMA grafting on the MWCNT. The PMMA-MWCNT experienced a weight loss of about 24% owing to the thermal decomposition of the PMMA bonded to the MWCNT.

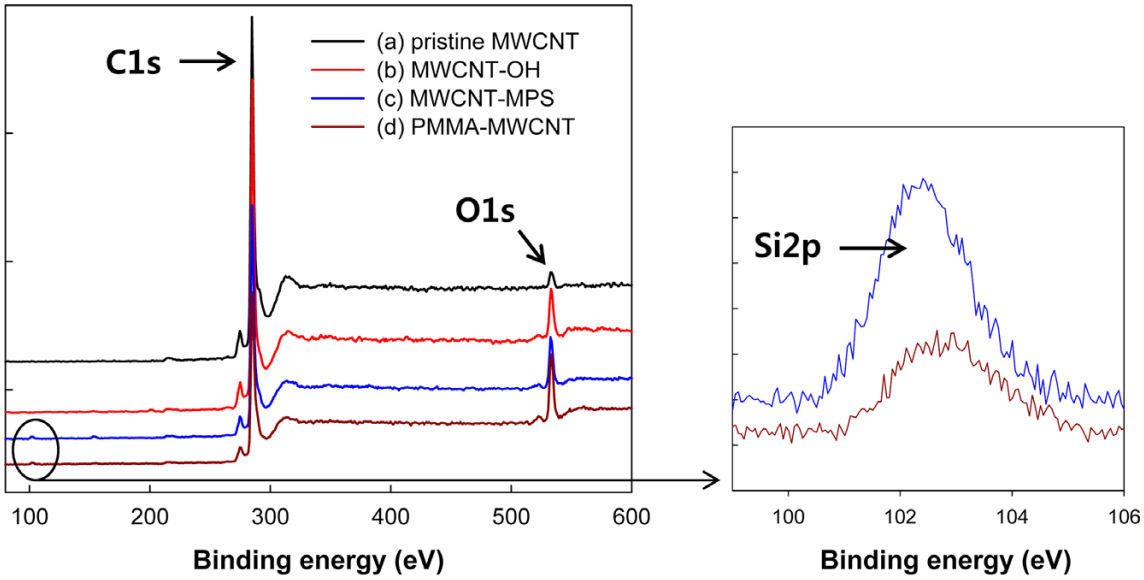

Figure 3. XP spectra of pristine and modified MWCNTs.

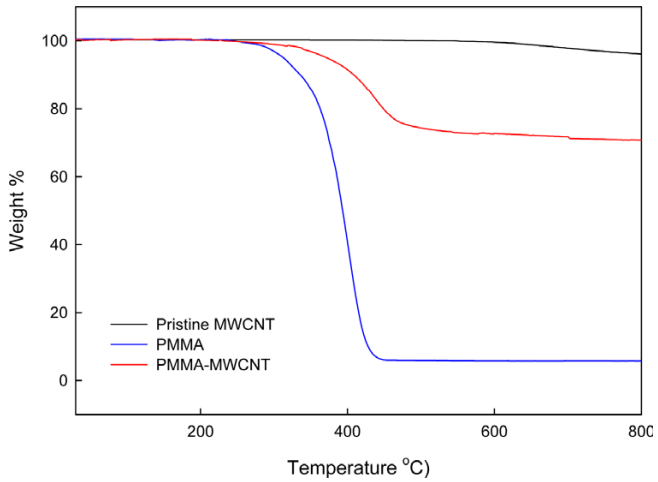

Figure 4. TGA thermograms of MWCNT, PMMA, and PMMA-MWCNT.

Figure 5 shows FE-SEM and HR-TEM microphotographs of the MWCNT and PMMA-MWCNT. The diameter of the PMMA-MWCNT increased to 50 nm and the MWCNT surface became rough as a result of the PMMA grafted on the MWCNTs. These results indicate that PMMA-MWNCT containing about 24 wt% of PMMA were produced.

4.2. Adhesion energy at the PC and MWCNT interface

The methods commonly used for the measurement of contact angles on planar surfaces cannot be applied to measure the contact angles of the barrel-type PC droplets on MWCNT. The contact angle was evaluated from a cylindrical PC droplet on a MWCNT using generalized drop-shape analysis.[21,23] The shape of the PC aggregates that precipitated on the MWCNTs (Figure 6(a)) changed due to annealing. The pristine MWCNT was enclosed by the cylindrical PC droplets (Figure 6(b)), while PMMA-MWCNT were encapsulated by PC (Figure 6(c)) after annealing. The changes in the shape of PC droplets were not observed with annealing time when the annealing time is equal to or greater than 20 min. It means that PC droplet formed on the MWCNTs reaches equilibrium when the PC-covered MWCNTs were annealed at 310 °C for more than 20 min. The contact angles were estimated from five PC droplets by generalized drop-shape analysis, and then average value was reported. The measured errors did not exceed 3°. The contact angle of PC with a MWCNT, determined by generalized drop-shape analysis, was 22° and that of PC with a PMMA-MWCNT was 0°. According to Young's equation, the adhesion energy of PC and MWCNT is given by:[20]

$$W_a = \gamma_L(1+\cos\theta) \quad (1)$$

where γ_L and θ and are the PC surface energy and the PC contact angle with MWCNT, respectively. Note that the PC surface energy is 45 mJ/m^2.[26] The PC adhesion energy with a MWCNT was 86.7 mJ/m^2, while that with a PMMA-MWCNT was 90 mJ/m^2, which is the same as the cohesive energy of PC, thus indicating that the adhesion of PC to the PMMA-MWCNT was the best that can be attained for composites of PC and MWCNT. It is known that PC blend with PMMA is nearly miscible.[17,18] Therefore, chain entanglement of PC with PMMA grafted on MWCNT is expected to occur at the interface, and the strong adhesion of PC to PMMA-MWCNT at the interface was the result of the PC miscibility with PMMA.

The dispersion of MWCNT in the composite was examined in films prepared by solvent casting. The shear stress applied to

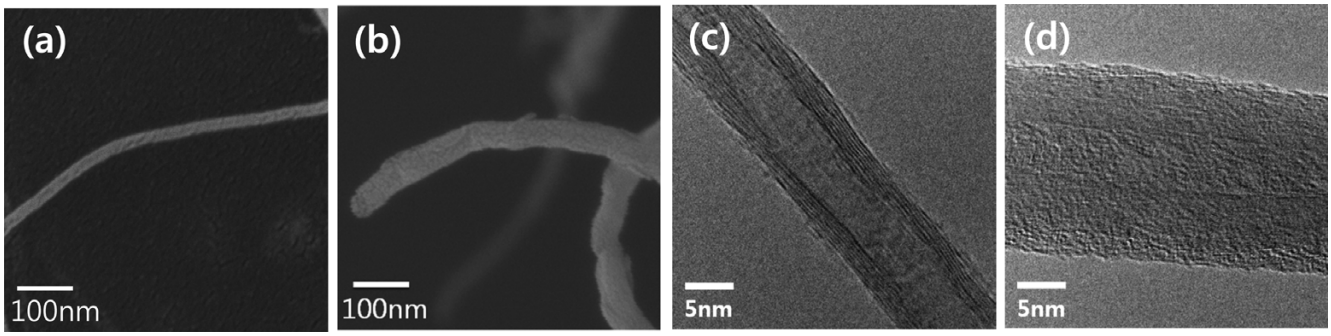

Figure 5. FE-SEM microphotographs of (a) MWCNT and (b) PMMA-MWCNT. HR-TEM microphotographs of (c) MWCNT and (d) PMMA-MWCNT.

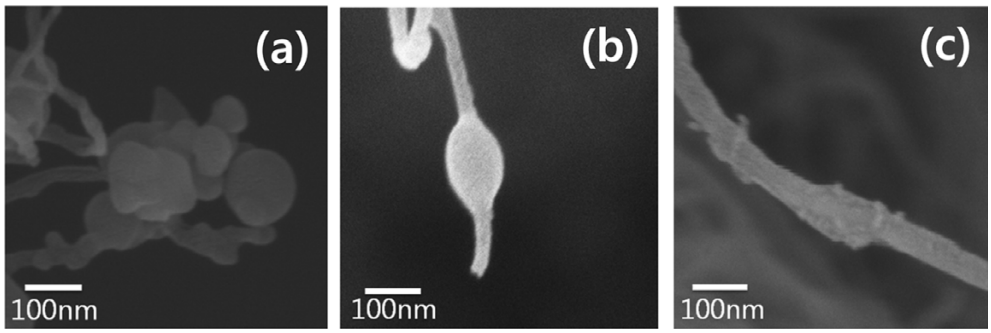

Figure 6. FE-SEM images of (a) PC precipitated on a MWCNT, (b) PC droplet formed on a MWCNT, and (c) a PMMA-MWCNT encapsulated by PC.

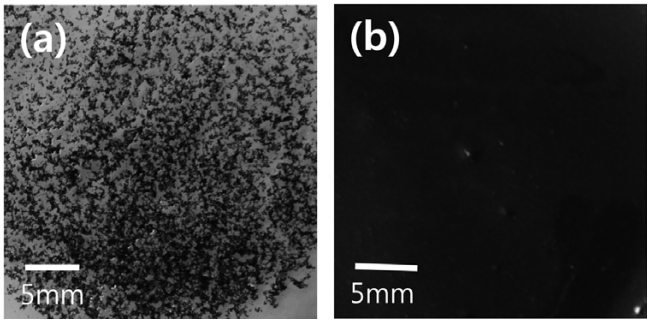

Figure 7. Photographs of PC composites with (a) MWCNT and (b) PMMA-MWCNT. Both composites contained 1 wt% of MWCNT.

the composite during melt extrusion improved the MWCNT dispersion in the composite. Since the effect of shear stress applied to the composite during melt extrusion on the MWCNT dispersion can be ignored by using solvent-cast films, The films prepared by solvent casting were used in examining MWCNT dispersion. Figure 7 shows the dispersion of MWCNT and PMMA-MWCNT in the composites. The dispersity of PMMA-MWCNT in the PC composite with PMMA-MWCNT was better than that of MWCNTs in the PC composite with MWCNT, indicating that the better adhesion of PMMA-MWCNT to PC resulted in better PMMA-MWCNT dispersion in the composite.

Figure 8 shows changes in tensile properties of the PC with MWCNT and PMMA-MWCNT as functions of the MWCNT content. The tensile strength and modulus of the composites increased with increasing MWCNT content. The tensile strength and modulus of the PC/PMMA-MWCNT composite were higher than those of the PC/MWCNT composite at a fixed composition. Figure 9 shows the fracture surfaces of the composites under liquid nitrogen conditions. The MWCNT was finely dispersed without MWCNT agglomeration in both composites. The fine dispersion of MWCNT in the composite might have resulted from the shear stress applied during melt extrusion. However, the adhesion of PMMA-MWCNT and PC at the interface was better than that of MWCNTs and PC. As shown in Figure 9, the PMMA-MWCNT was still wrapped with the polymer at the fracture surface, indicating that the load transfer between PC and the PMMA-MWCNT at the interface occurred more efficiently than that between PC and the MWCNT. The higher PC adhesion with PMMA-MWCNT resulted in the higher mechanical strength of the PC composite with PMMA-MWCNT.

As shown in Figure 10, the electrical conductivity of the composite was increased abruptly when the PC composites with MWCNT and PMMA-MWCNT contained about 1 and 0.7 wt% of MWCNT, respectively. This result indicates that that MWCNT

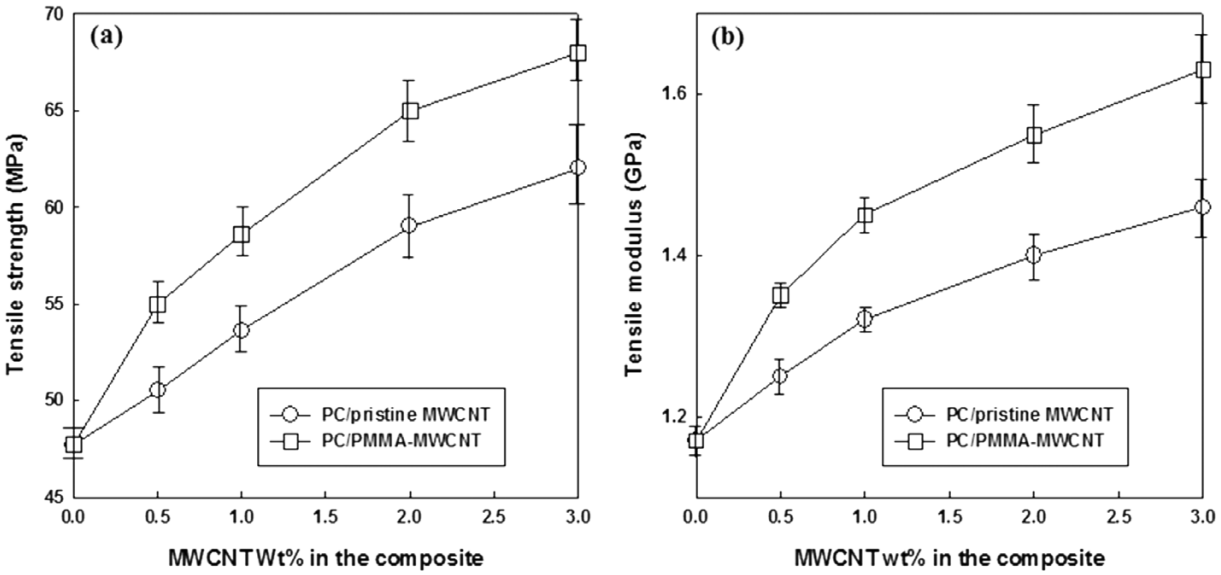

Figure 8. (a) Tensile strength and (b) tensile modulus of the PC composites with MWCNT and PMMA-MWCNT as functions of the MWCNT content.

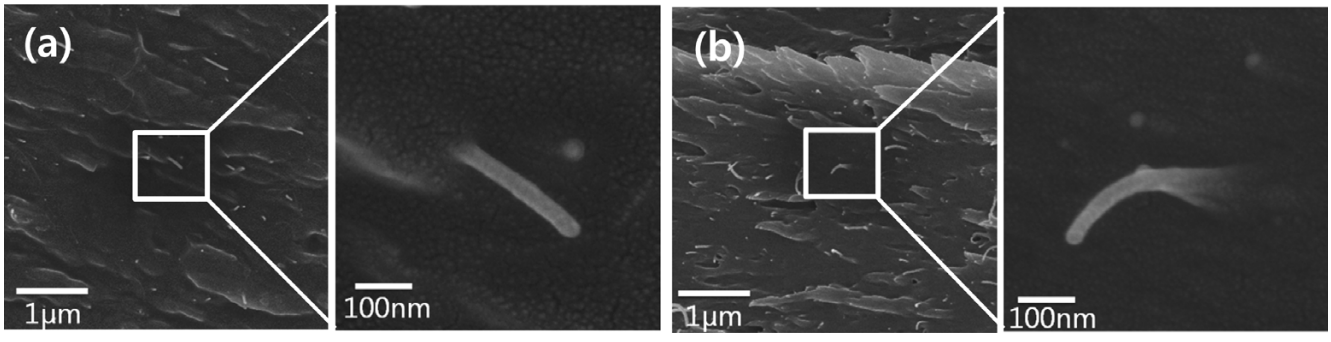

Figure 9. The fractured surface images of the PC composites with (a) MWCNT and (b) PMMA-MWCNT. Note that composites contain 1 wt% of MWCNT.

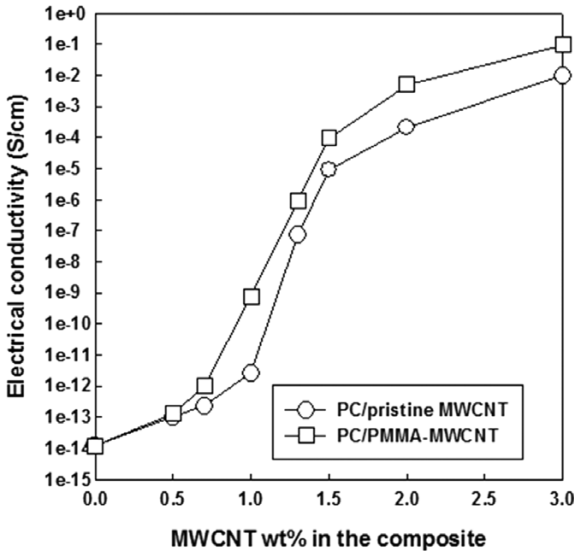

Figure 10. The electrical conductivities of the PC composites with MWCNT and PMMA-MWCNT as functions of the MWCNT content.

content required to form the network was lower in the PC/PMMA-MWCNT composite than in the PC/MWCNT composite owing to the improved dispersion of PMMA-MWCNT in the former. As a result, the conductivity of the former was higher than that of the latter at a fixed MWCNT content.

5. Conclusions

MWCNT with grafted PMMA was produced to improve the mechanical and electrical properties of the PC composites with MWCNT. PMMA-MWCNT was prepared by reacting the monomer MMA with vinyl groups in MWCNT-MPS. The formation of PMMA-MWCNT was explored with FT-IR, XPS, FE-SEM, HRTEM, and TGA analyses. The PC adhesion energy with the MWCNT was estimated by calculating the PC contact angle on the MWCNT surface by using generalized drop-shape analysis. The PC adhesion energy with the PMMA-MWCNT was higher than that with the MWCNT. In particular, the adhesion energy of PC and the PMMA-MWCNT was the same as the cohesive energy of PC, representing the best adhesion that can be achieved in the PC/MWCNT composites. This strong adhesion resulted from the chain entanglement of PC with PMMA grafted on the MWCNT owing to the miscibility of PC with PMMA. The PMMA-MWCNT dispersion in the PC/PMMA-MWCNT composite was also better than MWCNT dispersion in the PC/MWCNT composite. The tensile strength and electrical conductivity of the PC/PMMA-MWCNT composite were higher than that of with the PC/MWCNT composite at a fixed composition. In conclusion, the composites of PC with MWCNT having improved adhesion at the interface, MWCNT dispersion, tensile strength, and electrical conductivity could be fabricated by using PMMA-MWCNT.

References

(1) M. M. J. Treacy, T. W. Ebbesen, and J. M. Gibson, *Nature*, **381**, 678 (1996).
(2) M. S. Dresselhaus, G. Dresselhaus, and R. Saito, *Carbon*, **33**, 883 (1995).
(3) B. Fiedeler and F. H. Gojny, *Compos. Sci. Technol.*, **31**, 3115 (2006).
(4) P. Potschke, T. D. Fornes, and D. R. Paul, *Polymer*, **43**, 3247 (2002).
(5) N. G. Sahoo, S. Rana, J. W. Cho, L. Li, and S. H. Chan, *Prog. Polym. Sci.*, **35**, 837 (2010).
(6) S. M. Park, M. H. Kim, and O. O. Park, *Macromol. Res.*, **24**, 777 (2016).
(7) W. S. Choi and S. H. Ryu, *Colloid Surf. A*, **375**, 55 (2011).
(8) K. H. Kim and W. H. Jo, *Carbon*, **47**, 1126 (2009).
(9) S. C. Roh, E. Y. Choi, Y. S. Choi, and C. K. Kim, *Polymer*, **55**, 1527 (2014).
(10) M. Liebscher, T. Gartner, L. Tzounis, M. Micusik, P. Potschke, M. Stamm, G. Heinrich, and B. Voit, *Compos. Sci. Technol.*, **101**, 133 (2014).
(11) E. Y. Choi, J. Y. Kim, and C. K. Kim, *Polymer*, **60**, 18 (2015).
(12) D. Fretag, U. Grigo, P.R. Muller, W. Nouvertne, Polycarbonates, G. Menges, in: M. B. Overberger, G. Menges (Eds.), in *Encyclopedia of Polymer Science and Engineering* John Wiley & Sons, New York, 1988, Vol. 11, pp 648-718.
(13) S. Pande, A. Chaudhary, D. Patel, B. P. Singh, and R. B. Mathur, *RSC Adv.*, **4**, 13839 (2014).
(14) S. Kumar, B. Lively, L. L. Sun, B. Li, and W. H. Zhong, *Carbon*, **48**, 3846 (2010).
(15) C. K. Kim and D. R. Paul, *Polymer*, **33**, 4941 (1992).
(16) G. Wildes, H. Keskkula, and D. R. Paul, *Polymer*, **40**, 5609 (1999).
(17) M. Nishimoto, H. Keskkula, and D. R. Paul, *Polymer*, **32**, 272 (1991).
(18) M. H. Kim, J. H. Kim, C. K. Kim, Y. S. Kang, H. C. Park, and J. O. Won, *J. Polym. Sci., Part B*, **37**, 2950 (1999).
(19) E. Y. Choi, S. W. Kim, and C. K. Kim, *Compos. Sci. Technol.*, **132**, 101 (2016).
(20) T. Young, *Philos. Soc. Lond.*, **95**, 65 (1805).
(21) B. J. Carrol, *J. Colloid Interface Sci.*, **57**, 488 (1976).
(22) B. Song, A. Bismarck, R. Tahhan, and J. Springer, *J. Colloid Interface Sci.*, **197**, 68 (1998).
(23) M. Q. Tran, T. Cabral, M. P. Shaffer, and A. Bismarck, *Nano Lett.*, **8**, 2744 (2008).
(24) S. C. Roh, J. Kim, and C. K. Kim, *Carbon*, **60**, 317 (2013).
(25) M. Ferriol, A. Gentilhomme, M. Cochez, N. Oget, and J. L. Mieloszynski, *Polym. Degrad. Stab.*, **79**, 271 (2003).
(26) J. Brandrup, E. H. Immergut, and E. A. Grulke, in *Polymer Handbook*, 4th ed., John Wiley & Sons, Inc., New York, 1999, Chapter VI, p 531.